



Structural And Service Performance of Composite Slabs with High Recycled Aggregate Concrete Contents

Fetih Kefyalew,¹ Thanongsak Imjai,^{1,*} Reyes Garcia² and Boksun Kim³

Abstract

This study investigates the structural and serviceability performance of composite slabs cast with recycled aggregate concrete (RAC). Fifteen slabs (2.0 m by 1.0 m and 0.15 m thick) were tested: five in four-point bending up to failure, five to examine vertical deflections after 90 days of sustained loading, and five to examine human-induced vibrations. Different contents of coarse and fine recycled concrete aggregates (RCA) were examined (0%, 25%, 50%, 75% or 100%). The results from the four-point bending tests indicate that the use of RCA reduced the flexural capacity only marginally (by 7% for slabs with 100% RCA), but it reduced the energy absorption of the slabs more significantly (by up to 22%). The vertical deflections of the slabs after 90 days of sustained loading was similar, regardless of the level of RCA replacement. The results from the human-induced vibration tests show that all the slabs met the serviceability limits in current Eurocode 5, which indicates that RAC with high 100% of RCA is suitable for the construction of composite slabs. Finite element analyses (FEA) using Abaqus® provided further insight into the serviceability performance of the slabs. The FEA results show that the vibration performance of the slabs was mainly affected by their span length. The vibration frequencies of the slabs decreased (by up to 29.2%) as the span increased from 6m to 12m. This article presents new experimental data and insights into the structural and serviceability behaviour of composite slabs cast with 100% RCA, which are scarce in the existing literature. Hence, it contributes towards a better understanding on the behaviour of composite slabs cast with RAC. This in turn can encourage a more efficient use of resources in construction.

Keywords: Recycled Aggregate Concrete; Composite slabs; Vibrations; Serviceability; Metal deck.

Received: 02 October 2023; Revised: 09 November 2023; Accepted: 13 November 2023.

Article type: Research article.

1. Introduction

Composite structures are extensively used in the construction industry.^[1,2] Particularly, multi-storey steel-framed buildings are commonly built with composite floor systems with metal decking due to their lightweight, low cost, and quick construction. Composite floors typically comprise of a concrete slab cast on a metal deck supported on steel beams.^[3] The metal deck serves as stay-in-place formwork on floor systems, or as a structural enclosing for roofs.^[4] In recent years, the construction industry in Southeast Asia has been trying to

adopt circular economy practices, as well as searching for alternatives to use recycled materials from construction. In particular, the use of recycled aggregate concrete (RAC) in composite slabs has been identified as a very feasible structural option to make more efficient use of resources.^[5,6] Past studies^[7,8] have also demonstrated that good quality natural aggregate (NA) is less available in various places globally. Consequently, the cost of aggregate is steadily increasing, thus compelling the construction industry to find alternative aggregate sources to use in concrete production. There is indeed a significant demand for aggregates in Southeast Asian countries, driven by ongoing development and extensive infrastructure projects in the region. The utilization of Recycled Concrete Aggregate (RCA) in construction is essential in this context to address environmental concerns and promote sustainable construction practices.

The construction industry generates a huge amount of

¹ School of Engineering and Technology, Walailak University, Nakhon Si Thammarat, 80160, Thailand.

² Civil Engineering Stream, School of Engineering, University of Warwick, Coventry, CV4 7AL, UK.

³ School of Engineering, Computing and Mathematics, University of Plymouth, Plymouth, PL4 8AA, UK.

*Email: thanongsak.im@wu.ac.th (T. Imjai)

construction and demolition waste (C&DW).^[9-12] In terms of statistics, it is important to highlight that annually, more than 6 billion tons of CDW are deposited in landfills across the globe. Approximately 35% of the total CDW generated is sent to landfills without undergoing additional treatment. Nevertheless, there is a growing effort to promote recycling and reuse practices for CDW.^[13,14] In the meantime, the demand for raw materials used as concrete aggregate is around 2.7 billion tons annually across the EU,^[15] 900 million tons annually across the USA,^[16] and 700 million tons annually across Brazil,^[17] 60 million tons annually across the South East Asia.^[18,19] A large proportion of this C&DW corresponds to concrete that, if properly recovered and sorted, can be used as recycled concrete aggregate (RCA) in the production of new RAC elements.^[20-23] Previous studies have investigated the structural performance of RAC slabs. For instance, Zhu *et al.*^[24] studied experimentally the flexural performance of composite slabs cast with RAC. Different slab thicknesses and coarse RCA contents (up to 100%) were investigated. The results show that an increase in RCA contents reduced the ultimate capacity of the slabs by up to 15%. Zhang *et al.*^[25] investigated the long-term shrinkage behaviour of continuous RAC composite slabs. It was reported that non-uniform shrinkage induced deflection accounted for 47-73% of the overall deflection of slabs, and that RAC increased the total slab deflection by 31-77%. Zhang *et al.*^[26] also examined the interfacial bond behaviour of composite slabs through pull-out tests. They conducted experiments on fifteen slab specimens, considering variables such as the replacement ratios of RCA (0%, 50% and 100%), different water-to-cement ratios (0.31, 0.45 and 0.60), different metal deck thicknesses (0.8 mm, 1.0 mm and 1.2 mm), as well as different deck rib heights (48 mm and 65 mm). Second mode of failure was observed, and penetrating cracks were observed due to the different bonding strengths of the eversion and embedded edges, which induced a torsional moment in the concrete component. The results of their investigation revealed that the failure mode of composite slabs remained consistent regardless of the RCA content. However, reducing the steel deck rib heights led to an increased occurrence of cracks in the failed slabs. Cold-formed profiled composite slabs have greater strength to weight ratios when compared with traditional concrete slabs.^[27] Additionally, the incorporation of RCA resulted in a decrease in the ultimate bond stress ranging from 4% to 20% and a reduction in elastic stiffness between 8% and 14%, caused by a large number of cracks due to weaker bond compared to normal reinforced concrete. It was observed that the influence of RCA was linked to other parameters examined in the study, such as deformation, elastic stiffness and energy dissipation.

Furthermore, the model proposed by Zhang *et al.*^[5] was accurate at predicting the bond-slip behaviour of metal-RAC composite slabs.

Cui *et al.*^[28] investigated the flexural performance of RAC composite slabs using Abaqus® software. It was reported that the performance of slabs was heavily influenced by the coarse RCA contents and slab thickness, but also by the shape and thickness of the metal deck profile. Moreover, slabs with trapezoidal metal deck profiles with 0.8mm thickness had 6% more flexural capacity than counterpart slabs with re-entrant profiles. More recently, Wang *et al.*^[29] used nonlinear thermo-mechanical finite element (FE) models in Abaqus® to predict the long-term behaviour of RAC composite slabs. Wang *et al.* indicate that composite slabs with 100% RCA exhibited 45.5% and 10.75% increments in the maximum mid-span deflection and support bending moment compared to those with the NAC, respectively. In spite of the above findings, recent studies^[30-32] have identified that limited research has examined the structural performance of RAC composite slabs with high RCA contents (e.g. 100% of both coarse and fine RCA). Particularly, more experimental data are deemed necessary to produce practical design aids for structural elements cast with RAC.^[33]

Excessive vibrations in low-dampened lightweight slabs can result in discomfort to a building's occupants. The most prevalent type of vibrations in slabs is induced by human walking.^[34] Vibrations of floors with natural frequencies below about 10 Hz are more likely to cause discomfort to occupants.^[35-37] In comparison to typical reinforced concrete slabs spanning in two-ways, composite floor decks often behave as a one-way system, and this makes them more susceptible to vibrations. The vibration of composite slabs also depends heavily on the stiffness of their components. In particular, the relatively low stiffness of RAC is expected to increase vibrations that can lead to occupants' discomfort. As a result, it is necessary to investigate the serviceability performance of RAC composite slabs subjected to human-induced vibrations as limited research exists on the subject.

This article examines experimentally and numerically the structural and serviceability performance of composite slabs cast with RAC. Fifteen slabs were tested: five in four-point bending up to failure, five slabs to examine their vertical deflections after 90 days of sustained loading, and five slabs to study human-induced vibrations. Different contents of coarse and fine RCA were examined (0%, 25%, 50%, 75% or 100% replacement). The results are discussed in terms of observed damage, failure modes, ductility, accelerations, mid-span deflections, and vibration performance in comparison to serviceability limits in current codes. This article presents new

experimental data and novel insights into the structural and serviceability performance of composite slabs cast with 100% RCA, which are scarce in the existing literature. Parametric FEA on Abaqus® are also performed to study the vibration performance of the tested slabs. The results reported in this article contribute towards a better understanding on the performance of composite slabs cast with RAC.

2. Experimental programme

2.1 Geometry of slabs and reinforcement

The floor system tested in this study consisted of a 150 mm thick slab cast on a trapezoidal metal deck of size 2.0m×1.0 m. Fig. 1a shows schematically the cross-section of the metal deck, which served as permanent formwork with the deck ribs running parallel to the long direction of the slab. The metal deck was of 0.8 mm thick galvanised steel with embossments on the ridge. The dimensions of the metal deck profile were $l_1=131\text{mm}$, $l_2=120\text{mm}$, $l_3=90\text{mm}$, $h_1=100\text{mm}$, and $h_2=50\text{mm}$ (see Fig. 1a). A mesh of Glass Fibre Reinforced Polymer (GFRP) bars of 4 mm diameter placed at 200 mm centres (Fig. 1b) was used as top internal reinforcement. GFRP bars were selected to maximise durability, since corrosion is a common issue in slabs of buildings built in Southeast Asia. The concrete cover of the GFRP mesh was 100 mm. Fig. 2 shows a view of the GFRP bars and metal deck just before casting.

The fifteen slabs were divided into three groups according to the type of test: 1) five slabs were tested in four-point

bending up to failure, 2) five slabs were tested to examine their vertical deflections during 90 days of sustained loading, and 3) five slabs were tested to study human-induced vibrations. Accordingly, each type of test comprised five slabs of the same size but incorporating different RCA contents.

2.2 Material properties and concrete mixes

Five mixes were produced using Portland cement Type I. Four of the mixes incorporated coarse and fine RCA, which was obtained by crushing old concrete cylinders and sieving them to size fractions of 20.9 mm and 18.6 mm. The properties of the natural aggregate and RCA used in the mixes are summarised in Table 1. In this table, natural aggregates are identified with an “N” letter, whereas RCA are identified with an “R”. Fig. 3a show the coarse and fine RCA used in this study. Likewise, Fig. 3b shows that the coarse and fine RCA matched well the gradation of the original natural aggregate being replaced in the mixes.

Table 2 summarises the concrete mix designs. The control mix (mix RAC0%) only had natural aggregates. The four RAC mixes adopted from Zhu *et al.*^[14] and Zhang *et al.*^[15] (RAC25%, RAC50%, RAC75%, RAC100%) had four different contents of RCA (25%, 50% 75%, 100%) which replaced the natural aggregates by weight. Table 3 presents the test results from six specimens, which were subjected to surface treatment with lime-cement. These specimens were tested in accordance with ASTM C09^[38] standards to assess compressive strengths

Table 1. Properties of coarse and fine natural aggregates and RCA.

Properties	Coarse aggregate			Fine aggregate	
	NC	RC#2	RC#1	NF	RF
Bulk specific gravity (SSD)	2.71	2.43	2.51	2.60	2.77
Unit weight (kg/m ³)	1730	1397	1425	1550	1400
Water absorption (%)	0.28	4.59	5.13	1.05	2.65
Moisture (%)	0.61	2.24	2.14	1.35	2.42
Fineness modulus	-	-	-	2.7	1.8
Max. size (mm)	19.1	18.6	9.8	4.76	4.70
Impact value (%)	10.15	13.4	12.5	-	-
Crushing value (%)	21.77	23.12	20.12	-	-
Residual mortar (%)	-	32.5	30.2	-	32.5

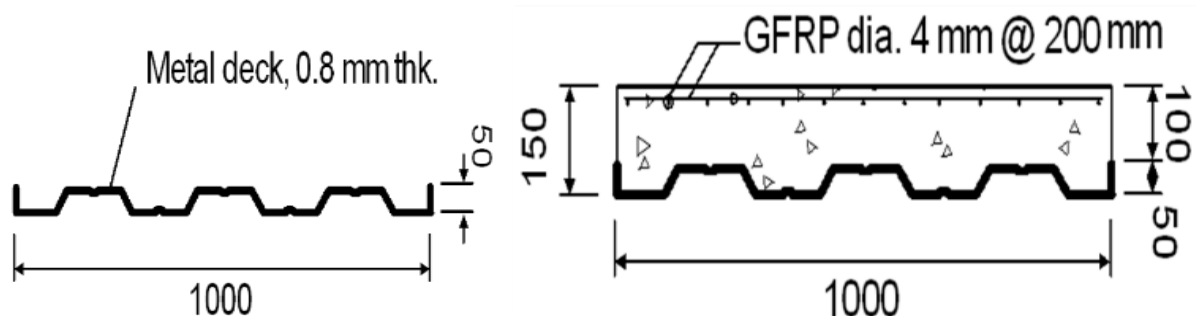


Fig. 1 Schematic view of (a) metal deck, and (b) cross section of concrete slab-deck system (units: mm).

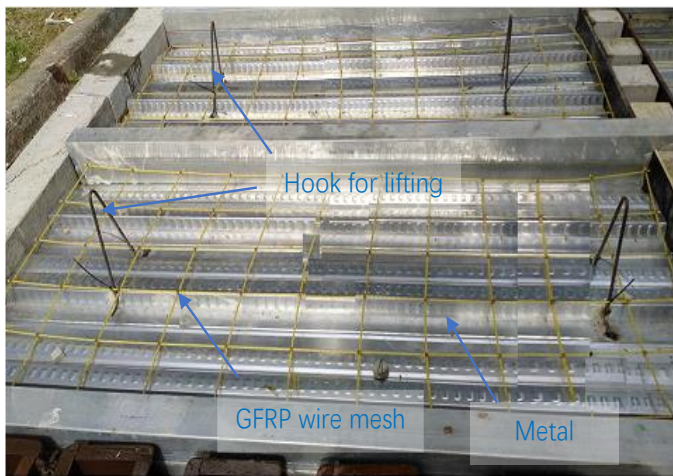


Fig. 2 View of GFRP mesh on metal deck before casting concrete.

obtained from 300mm high by 150mm diameter cylinders ($f_{c,cyl}$) and 150mm cubes ($f_{c,cu}$). Furthermore, tensile strength values from cylinders (f_t) and flexural strength data from 100mm x 100mm x 500mm prisms (f_b) were acquired through testing procedures in accordance with ASTM C496^[39] and ASTM C78,^[40] respectively. The table also includes standard variations (SD) of the different properties.

From the results shown in Table 2, it is evident that the slump value of a concrete mix tends to decrease as the proportion of Recycled Concrete Aggregate (RCA) increases. RCA particles typically have irregular shapes and rough textures, which hinder the flow of the mix by creating more resistance. The irregularity and reduced particle grading of RCA, when compared to natural aggregates, can also lead to

reduced workability. Additionally, the higher water absorption capacity of RCA can result in stiffer concrete mixes as water is absorbed, consequently leading to a lower slump value.

Table 2. Mix design of normal concrete (RAC0%) and four RAC mixes (amounts per m³).

Proportion	RAC0	RAC25	RAC50	RAC75	RAC100
	%	%	%	%	%
Cement (kg)	303	303	303	303	303
Water (kg)	129	129	129	129	129
w/c ratio	0.43	0.43	0.43	0.43	0.43
Natural fine	916	687	458	229	-
Fine RF (kg)	-	229	458	687	916
Natural	1028	771	514	257	-
Coarse RC	-	257	514	771	1028
Superplastici	1.07	1.07	1.07	1.07	1.07
Slump (mm)	91	86	82	78	75

The metal deck section had a nominal thickness of 0.8 mm. Six coupons were tested according to ASTM A370^[41] to obtain the following average mechanical properties: yield strength $f_y = 275$ MPa, ultimate strength $f_u = 337$ MPa, modulus of elasticity $E_s = 210$ GPa, and elongation at failure = 2.5%. Three GFRP bar samples were tested in direct tension and the following average mechanical properties were obtained: tensile strength $f_{tu} = 700$ MPa, modulus of elasticity $E_f = 43$ GPa, and ultimate strain $\epsilon_{fu} = 1.5\%$. The GFRP bars met the requirements in ACI 440.3R.^[42]

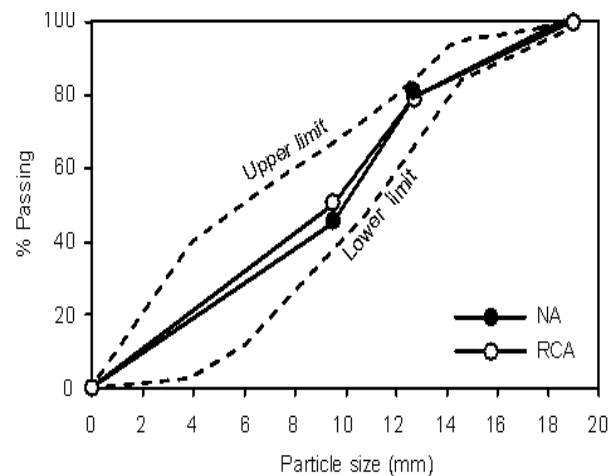
Table 3. Properties of normal concrete and RAC at 28 days.

Values	RAC0%	SD	RAC25%	SD	RAC50%	SD	RAC75%	SD	RAC100%	SD
$f_{c,cyl}$ (MPa)	34.6	1.8	32.1	1.7	32.3	2.3	30.7	1.9	28.3	2.1
$f_{c,cu}$ (MPa)	37.9	2.1	36.9	1.3	36.2	2.1	33.9	1.7	32.9	2.0
f_t (MPa)	4.1	1.7	3.5	2.1	3.3	1.8	3.0	2.4	2.9	1.6
f_b (MPa)	4.7	2.0	4.3	1.9	4.0	2.2	3.9	2.0	3.2	1.9



Fine RF Coarse RC#1 Coarse RC#2

(a)



(b)

Fig. 3 (a) Coarse and fine RCA, and (b) size distribution of natural aggregate and RCA.

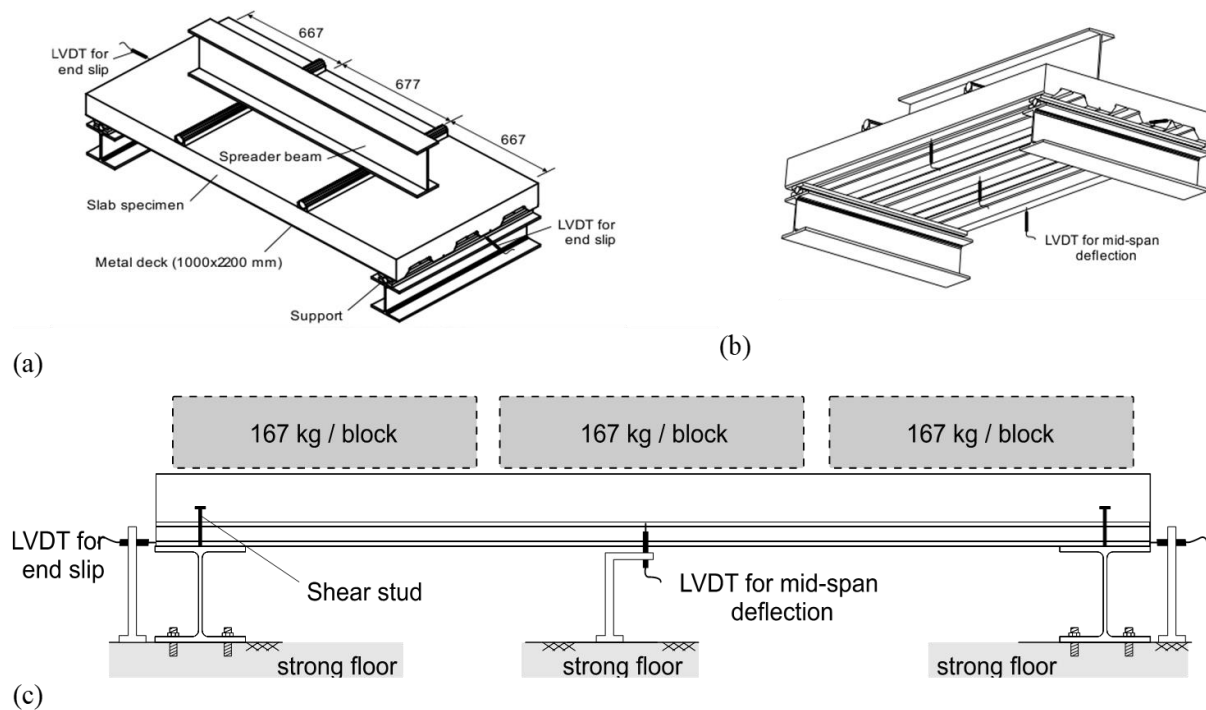


Fig. 4 Test setup and instrumentation for (a)-(b) four-point bending tests, and (c) 90-day sustained loading tests.

2.3 Test setup for short term loading tests and instrumentation

Five slabs (RAC0% control, RAC25%, RAC50%, RAC75%, and RAC100%) with shear studs welded for beam support were subjected to four-point bending tests until failure. The load was applied using a spreader beam and two pin rods laid parallel to the short direction of the slabs (see Fig. 4a). A hydraulic jack of 1,000 kN-capacity applied the load in a displacement control mode at a rate of 1.0 mm/min. Two LVDTs at both ends of the slab measured the end slip between the metal deck and the concrete slab. Similarly, three vertical LVDTs were installed at the bottom of the slabs to capture the average mid-span deflection (Fig. 4b). The load-deflection curves were recorded using a data acquisition system and the tests were carried out until the maximum load resisted by the slabs dropped by 20%.

2.4 Sustained loading arrangement

The vertical deflections of five composite slabs subjected to sustained load during 90 days was also investigated. Three LVDTs placed at the mid-span of the slabs and two at each end of the slab measured end slippage over the testing period. The deflection measurements started immediately after casting the concrete on the metal deck (which was already supported on steel I beams as shown in Fig. 4c), and measurements continued for 28 days until the concrete set. After these initial 28 days, three concrete blocks (167 kg each) were placed on the slabs, and the deflections were recorded for 32 days (Fig.

4c). The three blocks simulated a design live load of 2.5 kN/m², according to ACI 318.^[43] After 32 days, the concrete blocks were removed, and the deflections were monitored for another 30 days. Accordingly, the deflections were measured for a total of 90 days. Fig. 5 shows slab RCA100% during the test.

2.5 Human-induced vibration tests

Human-induced vibrations were produced on five slabs using the setup shown in Fig. 6, which was adopted from a previous study.^[44] One male (mass=58 kg, height=177 cm) and one female (mass=54 kg, height=160 cm) participants (m_1) were asked to walk on a 77 kg (m_2) treadmill (DOMYOS model T540C) placed on the slabs (see actual test setup in Appendix D). Three different types of vibration were considered: normal walking with an average walking speed of 5 km/h (as proposed by Shahid *et al.*,^[45]), brisk walking with an average walking speed of 10 km/h (according to Cavagna *et al.*,^[46]), and jumping. British Standard^[47] provides guidelines that specifically address vibration measurement or instrumentation. The participant’s speeds were measured using the speedometer of the treadmill. The maximum vibration values were measured in terms of gravitational acceleration ($g = 9.81 \text{ m/s}^2$) in accordance with British Standard.^[47] The accelerations were recorded using a $\pm 5.0g$ accelerometer (BDI A2000) placed at the bottom of the slabs. The accelerometer was mounted under the metal deck following ISO 2631-2^[48] and ISO 4866^[49] guidelines.



Fig. 5 Typical experimental setup for sustainable loading tests.

In this study, British Standard^[47] and ISO 2631-1^[50] was adopted as a benchmark for the human-induced vibration tests. The floor acceleration ranges summarised in Table 4 are deemed to be perceived by occupants in a building. ISO 2631-1^[50] suggests that, for a group of alert and fit people, the average perception threshold should be 0.015 m/s² (weighed peak acceleration). Accordingly, the occupants of residential buildings are likely to complain about vibrations if the floor accelerations are above 0.015 m/s². The values in Table 4 are later compared with the experimental results obtained from human-induced vibration.

3. Test results and discussion

3.1 Four-point bending tests

The initial load on the five slabs did not produce any significant cracking. At a load of around 20 kN (close to the yielding point), flexural cracks were clearly observed at the

location of the loading points (one crack below each point) and at the mid-span (one crack). The crack widths in the RCA100% slabs were the widest, being around 1.5 mm and 1.2 mm thick. In comparison, slab RCA0%, experience crack widths of 0.9 mm and 0.5mm only. Fig. 7 shows slab RCA100% during the four-point bending test, which is representative of the cracking

Table 4. Comparison of floor acceleration effects on building occupants (human perception to vibration).^[50]

Effect	Acceleration range
Imperceptible	$a < 0.005g$
Perceptible	$0.005 \leq a \leq 0.015g$
Annoying	$0.015g \leq a \leq 0.05g$
Very annoying	$0.05g \leq a \leq 0.15g$
Intolerable	$0.15g < a$

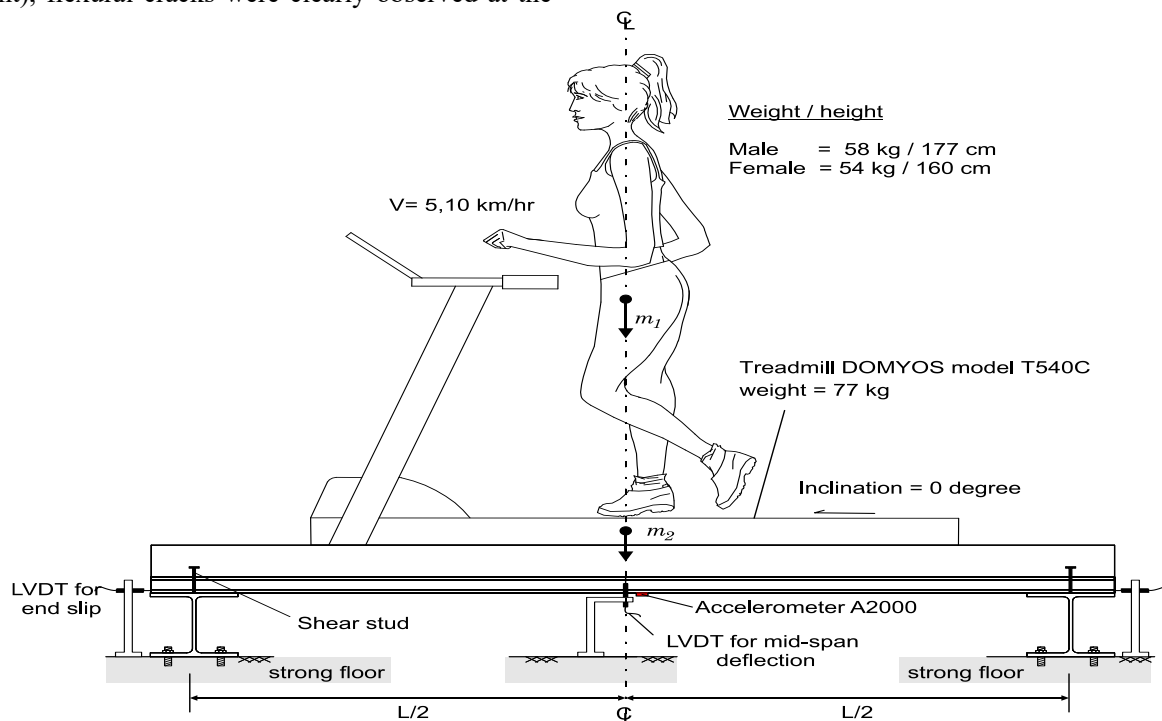


Fig. 6 Setup of human-induced vibration tests and position of a treadmill on the tested slab.

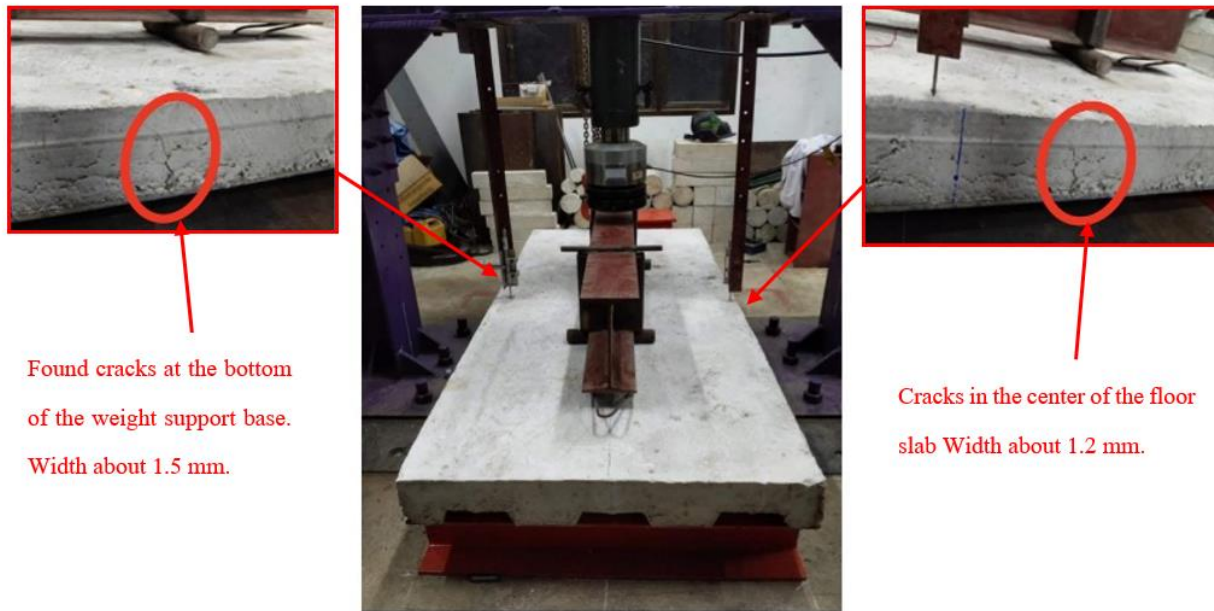


Fig. 7 Cracks observed at yielding in a specimen RCA100%.

observed in the rest of the slabs. Failure of the slabs was dominated by yielding of metal profile and crushing of concrete at the top of the slab.

Figure 8a compares the load versus mid-span deflection curves of the five slabs, whereas Fig. 8b shows the corresponding load versus (average) end slip curves. The results in Fig. 8a show that yielding started at approximately 22 kN for all slabs. In this study, the yielding point is defined as intersection point between the initial slope of the curves and their plateau. Fig. 8 also shows that the load vs mid-span deflection curve of slabs RCA0% (control) and RCA25% is practically the same. These results are consistent with past studies that suggest maximum RCA replacement levels of 20–25% so that RAC can retain the strength and workability of

normal concrete.^[51,52] This is also in line with current design codes^[53-55] which limit the maximum replacement of coarse RCA to 20% in new structural RAC. Note that the curves in Fig. 8a are only shown up to the ultimate load (P_u) at which the maximum capacity of the slab P_{max} dropped approximately by 20%.

Figure 8b shows that end slip occurred even at relatively low levels of load, thus indicating relative movement between the concrete slab and the metal deck. After yielding, end slips increased rapidly but the load remained relatively constant until failure of the slabs occurred. The results also show that end slip tended to increase as the RCA contents increased. The end slip can be mainly attributed to debonding between the concrete slab and the metal deck. The results in Fig. 8b

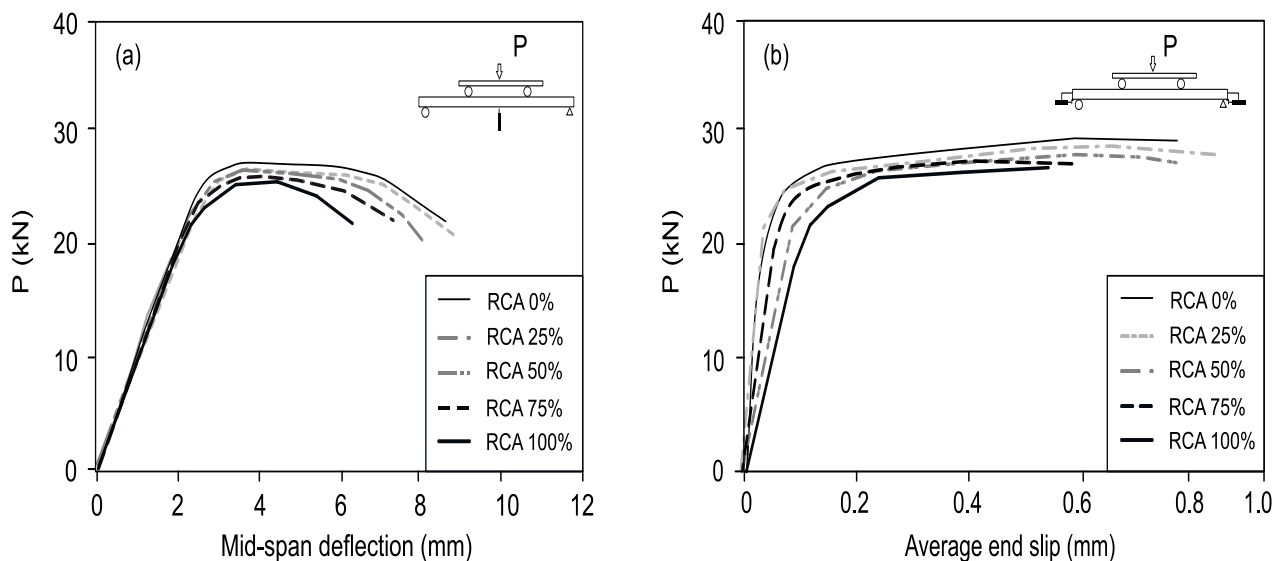


Fig. 8 Results from slabs with different levels of RCA: (a) load vs mid-span deflection curves, and (b) load vs end slips.

suggests that end slip is more likely to occur at high RCA contents (RCA50% and above). The recorded end slip was between 0.5-0.9 mm at P_{20} .

Table 5 summarises the results obtained from the four-point bending tests. It is shown that, compared to control slab RCA0%, the maximum load capacity P_{max} reduced by 2%, 2%, 3% and 7% in slabs RCA25%, RCA50%, RCA75%, and RCA100%, respectively. These results are slightly lower than those reported by Zhu *et al.*^[24] who found that the capacity of slabs with 100% RCA reduced by 15%. Moreover, the ultimate deflection Δ_u of slabs RCA25%, RCA50%, RCA75% and RCA100% increased by 4%, 3%, 4% and 20% when compared to that of slab RCA0%. The latter effect can be attributed to the lower stiffness of RAC compared to normal concrete.

In this study, the displacement ductility (μ) is calculated as the deflection ratio Δ_u/Δ_y . The results in Table 5 indicate that, compared to the control slab RCA0%, the ductility of the rest of the RCA slabs reduced between 14% and 17%. The initial stiffness at the yield point (K_e) of slab RCA100% was also reduced by 12% with respect to RCA0%. Table 5 also shows that the energy absorbed by the slabs (calculated as the area under the load-deflection curve) dropped by up to 22% in slab RCA100% compared to RCA0%. Overall, the above findings are in line with previous research that report that high RCA replacement contents reduced the capacity, ductility, stiffness and energy absorption of the slabs. Whilst the results from the four-point bending tests indicate that the use of RCA in composite slabs reduced their structural performance, the reduction is not severe even if all coarse and fine aggregates are fully replaced with 100% RCA. As a result, the use of RAC in composite slabs is deemed as a feasible option, as recently suggested by Zhang *et al.*^[5] However, further experimental evidence is necessary to confirm the findings presented in this study.

3.2 Sustained loading test results

Figure 9 presents the results obtained from the 90-day sustained loading tests. The results in Fig. 9a suggest that the

use of RCA in composite slabs (regardless of the RCA contents) changed the load-deflection behaviour after 90 days of sustained loading. Fig. 9b shows the maximum (Δ_{max}) and residual (Δ_r) deflections experienced by the slabs. It is shown that both Δ_{max} and Δ_r increased marginally but consistently with the RCA contents. Specifically, the maximum deflection (Δ_{max}) in slab RCA100% was notably 16.7% higher than that in slab RCA0%, indicating that the slab containing 100% RCA experienced slightly greater deformation under the applied load. Similarly, the residual deflection (Δ_r) displayed an increase, albeit of a smaller magnitude, with slab RCA100% exhibiting a 4.3% higher residual deflection compared to slab RCA0%. This suggests that even after the load was removed, the slab containing 100% RCA retained a slightly higher level of deformation compared to the slab without RCA. These findings emphasize the influence of RCA content on the deflection behavior of composite slabs, carrying implications for structural considerations and design choices in construction projects employing RCA as an alternative to normal aggregates. In spite of this, all slabs with RCA meet the deflection requirements in ACI 318-14^[43] requirements. Indeed, in ACI 318, the acceptable limit for long-term deflection of a simply supported reinforced concrete slab accounted for shrinkage and creep effect, is typically $L/350$ (L =span length). For a reinforced concrete slab with a clear span of 2000 mm, the acceptable long-term deflection limit would be $L/350 = 5.71$ mm. Accordingly, the test results for all slabs were under the maximum allowable deflection limit. It is important to note that additional tests are necessary to confirm these findings and evaluate the long-term performance (beyond 90 days) of other composite slabs with RCA.

3.3 Vibration test results

3.3.1 Floor acceleration

Figure A1 in Appendix A shows the acceleration measured during the tests on the RCA0% and RCA100% slabs, which are representative of the rest of the measured accelerations.

Table 5. Summary of four-point bending test and performance indices results on composite slabs.

Slab ID	P_{max} (kN)	P_u (kN)	Δ_u (mm)	Δ_y (mm)	μ	K_e (kN/m)	Energy (kN·mm)
RCA0%	27.0	21.6	4.20	2.3	1.83	10.48	187.9
RCA25%	26.5	21.2	3.64	2.3	1.58	10.08	180.2
RCA50%	26.4	21.1	3.62	2.3	1.57	9.95	171.1
RCA75%	26.1	20.9	3.60	2.3	1.56	9.61	164.9
RCA100%	25.2	20.2	3.50	2.3	1.52	9.21	147.2

Note: P_{max} = maximum load, P_u = ultimate load after a drop of 20% in P_{max} , Δ_u = deflection at P_{max} , Δ_y = deflection at yield point, μ = displacement ductility, K_e = initial stiffness of the load-deflection curve.

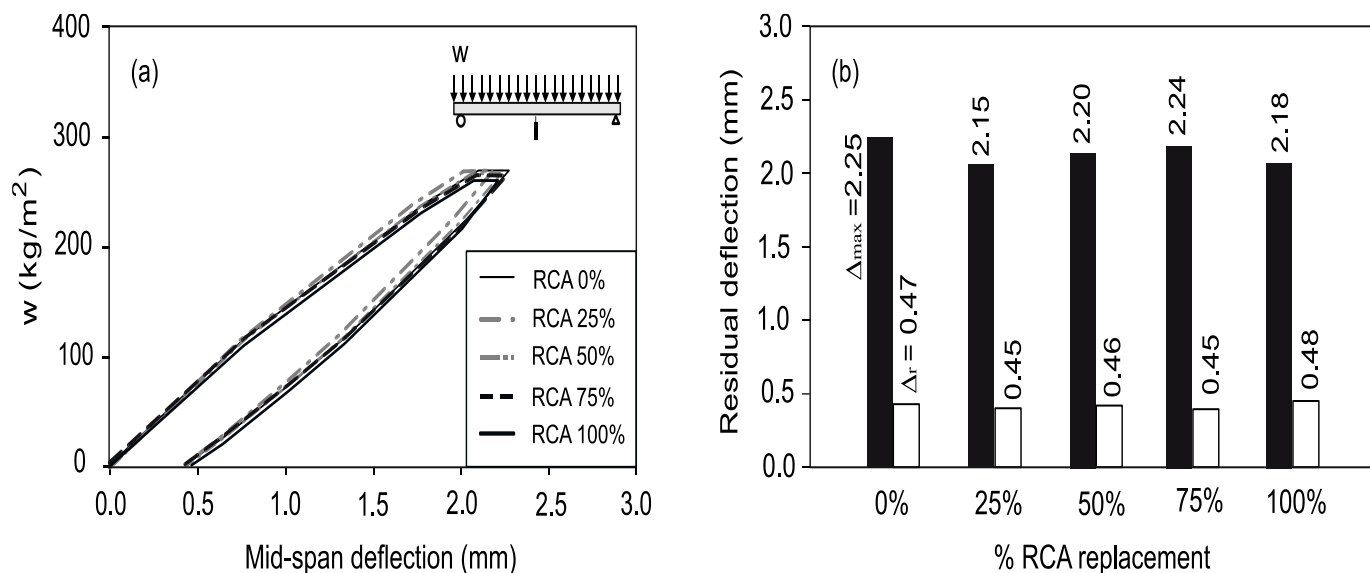


Fig. 9 Results from 90 day sustained loading tests: (a) load vs mid-span deflection, and (b) mid-span residual deflection.

The results in Figs. A1a-b show that, for both participants and for normal walking and brisk walking, all slabs remained below the maximum acceleration recommended in the standard (0.15g, according to Table 4). Conversely, Fig. A1c shows that the recommended acceleration (0.15g) was exceeded in the case of jumping, thus entering the “highly annoying” level shown in Table 4.

Figures 10a-b compare the maximum acceleration of the slabs subjected to normal walking (Fig. 10a), brisk walking (Fig. 10b), and jumping (Fig. 10c). The results in Figs. 10a-b show that the acceleration tended to increase with the walking speed of the participant. In the case of jumping (Fig. 10c), the acceleration of the slabs was above the “irritating” level (see Table 4). In general, the use of RCA in composite slabs led to higher accelerations during normal walking, brisk walking and jumping. Compared to the control slab RCA0%, the acceleration of slab RCA100% during normal walking, brisk walking and jumping was 19.1%, 9.1% and 8.5% higher, respectively. Despite of this, the vibration of slab RCA100% remained below the limits proposed in ISO 2631-2,^[48] thus confirming that the vibration performance of the slab was acceptable. These results suggest that high RCA contents (up to 100%) can be used in composite slabs without compromising the occupants’ comfort. Moreover, previous research^[56,57] has also indicated that the vibration performance of RAC slabs is similar to that of NAC slabs. This similarity can be attributed to the favourable damping behaviour of the RAC slabs.

3.3.2 Natural frequency

According to ISO 2631-2,^[47] the natural frequency of a floor should be above 8.0 Hz to remain within acceptable levels.

This is because occupants can experience vibration discomfort at low frequencies. A Fourier analysis was carried out using Matlab® to obtain the frequency responses of the slabs from the vibration measurements, as suggested by Davis *et al.*,^[57] Fig. 11 compares the natural frequency vs Root Mean Square (RMS) accelerations of slab RCA100% for both participants for normal walking (Fig. 11a), brisk walking (Fig. 11b), and jumping (Fig. 11c). Appendix B presents the results of the rest of the slabs. For RCA replacement level of 25%, 50%, 75%, and 100%, the vibrations experienced during normal walking also increased by 4.8%, 13.4%, 17.3%, and 24.3% respectively, over the control slab RCA0%. The same behaviour was observed for brisk walking and jumping where, compared to slab RCA0%, the vibration of slab RCA100% increased by 10.4% and 9.3% respectively. The results demonstrate a progressive trend in vibration amplification as the RCA replacement levels increased. The results for RCA100% slabs show that, for both participants, the natural frequencies for normal walking (5.15-5.78 Hz), brisk walking (8.28-8.95 Hz) and jumping (10.08-10.12 Hz) remained within an acceptable range of comfort for occupants. Accordingly, RCA is deemed as a feasible option to be used as a composite metal deck slab.

4. Finite element analyses of composite slabs

4.1 Model geometry, boundary conditions, and loading procedure

To provide further insight into the performance of the tested slabs, non-linear finite element analyses (FEA) were carried out on Abaqus® software.^[58] The analyses were performed with the inclusion of both material and geometric nonlinearities. The concrete of all slabs was modelled using 8-node linear brick elements, and C3D10M tetrahedron

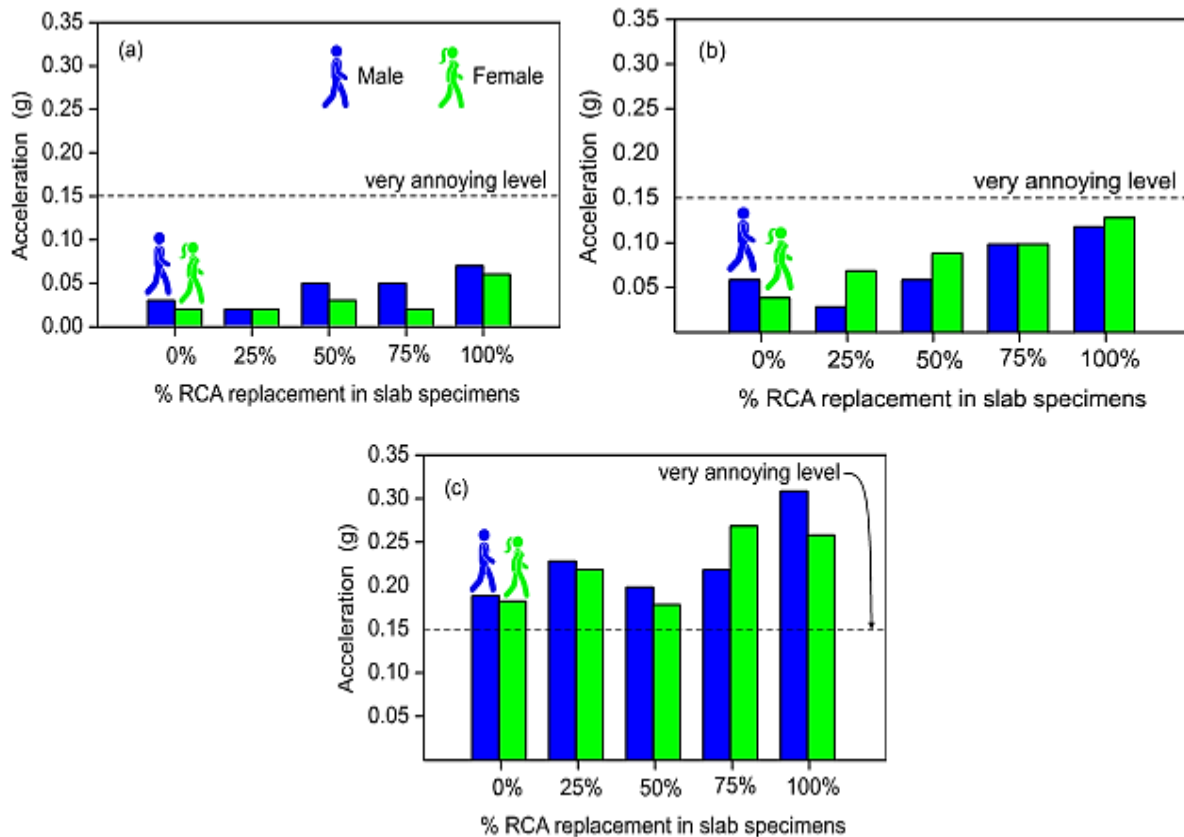


Fig. 10 Maximum acceleration of slabs subjected to (a) normal walking, (b) brisk walking, and (c) jumping.

elements (see Fig. 12) with a modified second-order integration scheme. The optimisation mesh sensitivity was performed, which resulted in a mesh size of 8 mm chosen for analysis. This function is automatically implemented by the software to minimise errors due to distortions during the analysis. The number of elements and nodes were 347,412 and 318,560 respectively. The material properties obtained from the laboratory tests and presented in Section 2.2 were used as input. The mean moduli of elasticity of the concretes were calculated using Eurocode 2.^[59] and were 33.2 GPa, 32.6 GPa, 32.1 GPa, 31.5 GPa and 30.1 GPa for mixes RAC0%, RAC25%, RAC50%, RAC75% and RAC100%, respectively. The Concrete Damage Plasticity (CDP) model is employed to describe the non-linear behaviour of concrete. It incorporates the stress-strain relationship for both tension and compression. In the compression section of the CDP model, a linear response is maintained until reaching the initial yield value (σ_{c0}). Beyond this point, the behavior shifts due to stress hardening, followed by strain-softening after surpassing the ultimate stress (σ_{cu}). In the tension zone of the CDP model, a linear elastic relationship is upheld until the failure stress value (σ_{t0}) is reached. Beyond this stage, the response exhibits softening stress-strain behavior, leading to the formation of microcracks. The GFRP bars were simulated using 2-node

truss (T3D2) embedded elements with two Gauss-Legendre integration points. Likewise, 4-node doubly curved shell (S4R) elements were used to simulate the metal deck. A linear stress-strain relationship was adopted for the GFRP bars. Since the main focus of the analysis was to examine the deflection of the slabs during service, perfect bond was assumed between the bars and the surrounding concrete. This was reasonable because there was no evidence of bond failures in the tested slabs. In many precast concrete elements however, bond-slip of the reinforcement can play an important role in the response, especially at high levels of load or after yielding of the reinforcement. The I beam supports of the experimental set-up were modelled using elastic C3D10M tetrahedron elements. The boundary conditions and loads were applied directly on the supports to avoid unrealistic stress fields in the slabs. The load was applied by direct displacement control at the mid-span of the slab. To model the concrete slab, the element size was optimised and varied where the irregular geometry was detected.

4.2 Comparison of the experimental results and FE predictions

4.2.1 Four-point bending tests

A damage index analysis was performed here. The damage

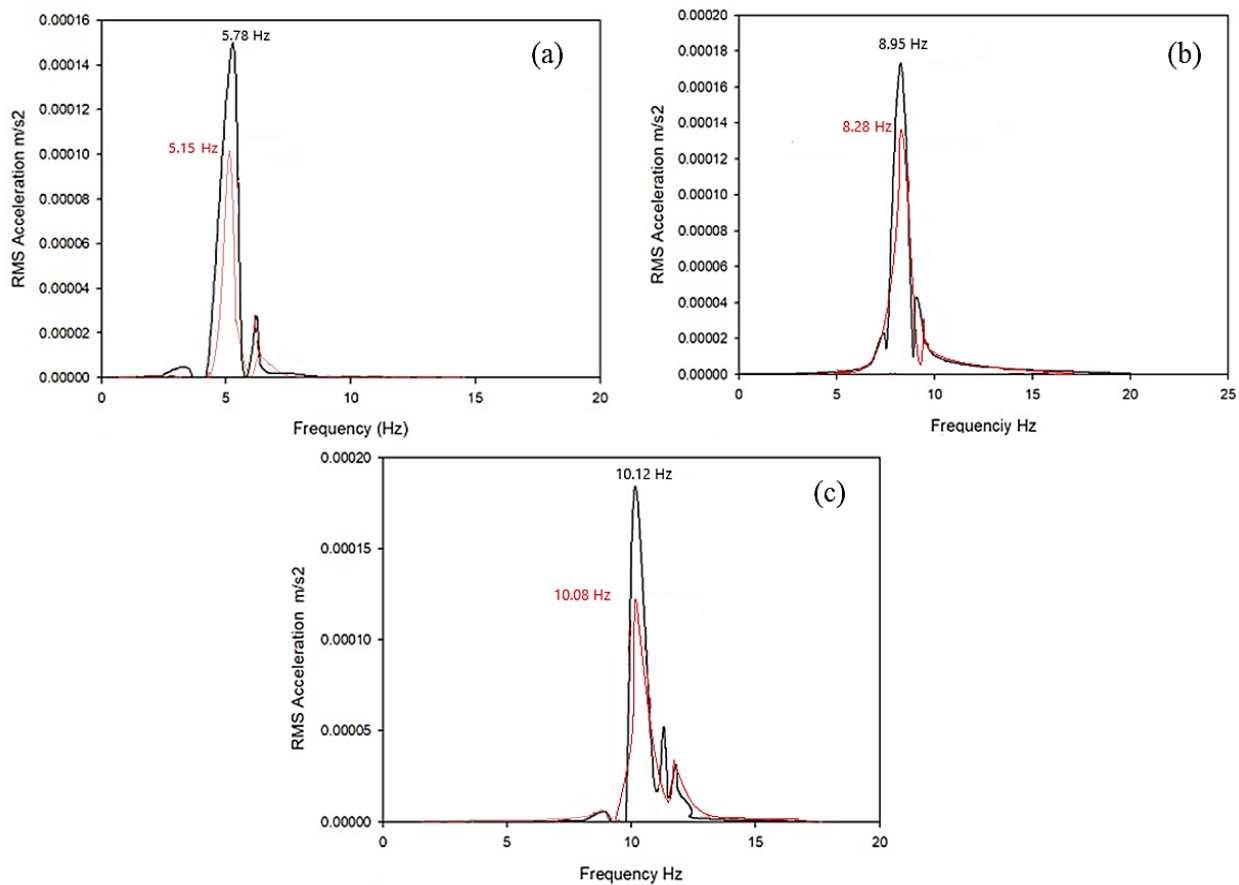


Fig. 11 Frequency response of slab RCA100% slab for (a) normal walking, (b) brisk walking, and (c) jumping.

index of concrete in Abaqus® is defined as a compressive damage (DAMGEC) and a tensile damage (DAMGET). Accordingly, cracks develop in concrete if the DAMGET value is above 1.0. Fig. 13a shows the cracking pattern of slab RCA50%, which is representative of the damage observed in the rest of the slabs. Fig. 13b shows that the results from Abaqus® agree well with the experimental observations, where three flexural cracks developed during the tests as

described previously in Section 3.1.

Table 6 compares the maximum load and mid-span deflection at maximum load of experimentally measured (EXP) values and those from FEA for different RCA replacement levels. The table also shows the percentage error, which are indicative of the accuracy of the ultimate load and mid-span deflection calculated by Abaqus®. The data in Table 6 show that, overall, the FEA results agree well (within an accuracy of

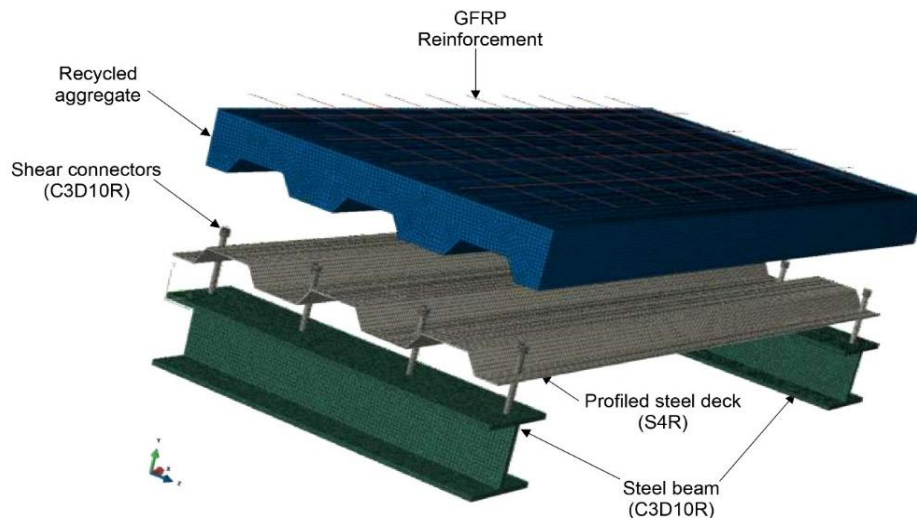


Fig. 12 Typical view of 3D model of slabs in Abaqus®.

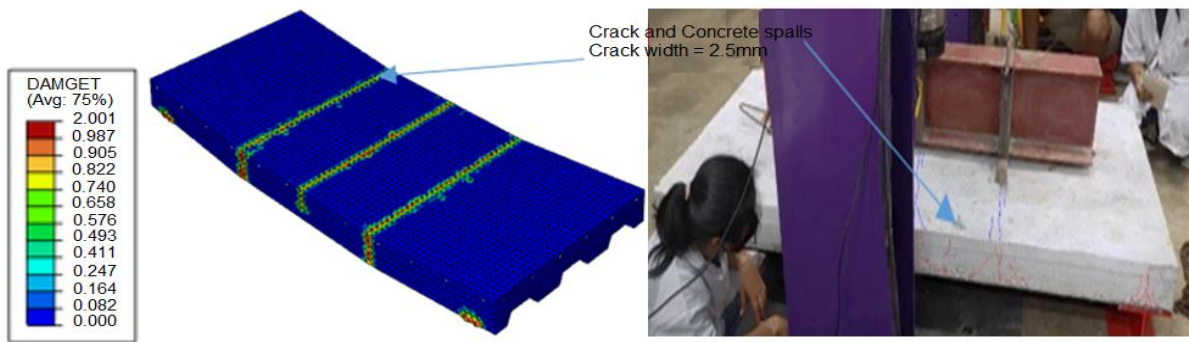


Fig. 13 (a) DAMGET crack analysis results, and (b) damage of slab RCA50% at P_{max} .

2 to 5%) with the experimental test results, suggesting that Abaqus® can capture well the load vs mid-span deflection curves obtained from the tests. Abaqus® is suitable to simulate the flexural capacity of the tested RAC slabs. The results in Fig. 14 confirms that

Table 6. Comparison of experimental values and FEA predictions for deflections at maximum load levels.

Slab ID	P_{max} (kN)			Δ_{max} (mm)		
	EXP	FEA	Error %	EXP	FEA	Error %
RAC0%	27.0	27.8	2.9	3.50	3.61	3.1
RAC25%	26.5	27.4	3.4	3.62	3.69	1.9
RAC50%	26.4	27.3	3.4	3.60	3.71	3.0
RAC75%	26.1	26.8	2.6	3.64	3.77	3.6
RAC100%	25.2	26.1	3.6	4.20	4.41	4.9

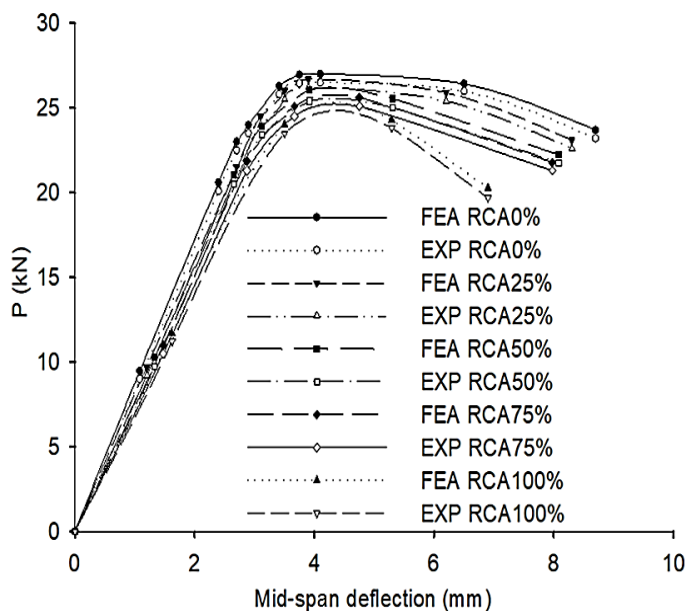


Fig. 14 Comparison of experimental deflections and predicted values obtained from finite element analysis.

4.2.2 Natural frequency

The results of a frequency analysis including modal shapes and natural frequencies for the first modes are depicted in Fig. 15. The first natural frequency of the slabs (f_1) varied depending on the RCA content, with values of 6.75 Hz, 7.15 Hz, 7.53 Hz, 8.15 Hz and 8.73 Hz for slabs RCA0%, RCA25%,

RCA50%, RCA75% and RCA100%, respectively. A comparison of FEA and experimental results (expressed as Prediction/Test ratios) indicate T/P values of 0.91, 0.94, 0.96, 1.01 and 1.05 for slabs RCA0%, RCA25%, RCA50%, RCA75%, and RCA100%, respectively, with an average T/P = 0.97 for all slabs. These results confirm that the numerical models and modelling approach in Abaqus® capture very well the dynamic behaviour of the tested slabs. As a result, such models are used to perform a parametric analysis to study the human-induced vibrations on longer spans of composite RAC slabs, as described in the following section.

4.3 Parametric analysis

The parametric analysis aimed to evaluate the influence of the slab thickness and span length on the vibration and comfort levels of occupants. The results from the parametric analysis are then compared with the acceptability levels of occupants' comfort, as suggested by Mast.^[60] Accordingly, the FEA models developed in the previous section were modified to account for the new slab geometries, Table 7 presents the spans and slab thicknesses selected for the parametric analysis, according to typical values recommended for design of composite floors of multi-storey buildings.^[61] In total, six FE models were created by considering two slab thickness (125 or 150mm) and three span lengths (6, 9 or 12m). Fig. C1 to C6

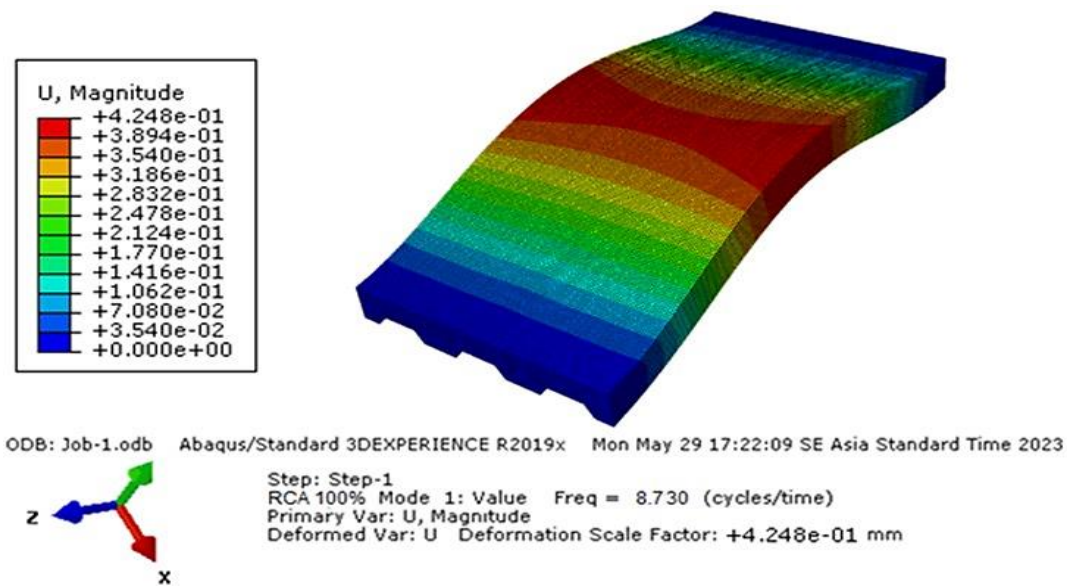


Fig. 15 Modal shape of RCA100% slab with $f_1=8.73$ Hz.

in Appendix C present the modal shapes of the models. The results indicate that the span was the major factor influencing f_1 , with a consistent decrease in f_1 as the span length increased. The slab thickness had a minor influence on f_1 , with an apparent reduction of f_1 with an increase in slab thickness.

Table 7. Models included in parametric analysis and first natural frequencies of RCA100%.

Model	Slab thickness (mm)	Span (m)	f_1 (Hz)
1	125	6	8.9
2	125	9	8.8
3	125	12	8.5
4	150	6	8.4
5	150	9	7.6
6	150	12	6.3

Table 8 presents a summary of the calculated first natural frequencies for the composite slabs with different RCA replacement levels. The table also includes the results from previous research conducted by Mast.^[60] The results in **Table 8** show that most of the models had natural frequencies that were within the recommended limits, with the exception of Model 3, which had a shorter span. The natural frequencies were in most situations below the limits recommended in past

studies.^[36] These findings further support the use of RAC as a suitable material for the construction of composite slabs. However, the results from the parametric analysis indicate that, in order to meet the serviceability criteria in ACI 318,^[43] the span length of slabs with 100% RCA should be below 12 m, and they should have a deck depth above 125 mm. Further parametric analyses are required to examine other case studies different to those investigated in this study.

The findings from this research, based on both experiments and numerical simulations, strongly support the effective use of Recycled Concrete Aggregate (RAC) in constructing composite slabs from both structural and serviceability perspectives. To fully embrace the potential of RAC, further investigations involving various types of RAC and diverse slab geometries should be conducted to validate these findings. Additionally, conducting human-induced vibration tests on longer-span RAC slabs with groups of participants is essential to gain deeper insights into their dynamic behaviour. This research holds broader implications for Southeast Asia, where the utilization of Recycled Concrete Aggregate (RCA) faces significant challenges linked to limited awareness, inadequate infrastructure, concerns about quality, and the need to adapt local construction practices. However, within these

Table 8. First natural frequencies of FEA models of slabs.

	Natural frequencies (Hz)					
	RCA0%	RCA25%	RCA50%	RCA75%	RCA100%	Mast ^[60]
1	5.32	6.53	7.67	8.14	8.7	8.8
2	5.17	6.32	7.41	7.79	8.6	8.8
3	4.87	5.91	7.28	7.63	8.5	8.7
4	4.73	5.73	6.97	7.42	8.4	8.7
5	4.54	5.54	6.79	7.25	7.6	6.9
6	5.32	5.32	6.53	7.11	6.3	7.0

challenges lie compelling opportunities, including contributing to environmental sustainability, conserving resources, and realizing long-term cost savings by reducing waste disposal. Thus, the research underscores the rationale for embracing RCA adoption. Despite potential initial costs associated with RCA, aligning with environmental regulations, mitigating waste management issues, and advancing long-term sustainability not only make it a valuable investment for the construction industry but also reflect a broader commitment to responsible and sustainable construction practices in the region.

5. Conclusions

This study investigates the structural and serviceability performance of composite slabs cast with recycled aggregate concrete (RAC). Fifteen slabs were tested: five in four-point bending up to failure, five to examine vertical deflections after 90 days of sustained loading, and five to examine human-induced vibrations. Different contents of coarse and fine recycled concrete aggregate (RCA) replacement were examined (0%, 25%, 50%, 75% or 100%). Finite element analyses (FEA) using Abaqus® provided further insight into the serviceability performance of the slabs. Based on the results presented in this study, the following conclusions can be drawn:

- The results from four-point bending tests indicate that the replacement of normal aggregate with RCA consistently decreased the capacity of RAC slabs, whereas it also increased their vertical deflections. Compared to a control slab cast with normal concrete (slab RCA0%), the maximum load capacity of a counterpart slab cast with 100% RCA (slab RCA100%) reduced by 7%. Moreover, the ultimate deflection of slab RCA100% increased by 20% when compared to that of slab RCA0%. These results highlight the need for careful evaluation of the use of RCA in concrete elements, particularly because high RCA replacement levels (above 75%) can reduce the structural performance of composite slabs.
- The results from the 90-day sustained loading tests show that the maximum (Δ_{max}) and residual (Δ_r) deflections experienced by the slabs increase with the amount of RCA replacement. Compared to slab RCA0%, the Δ_{max} and Δ_r of slab RCA100% increased by 16.7% and 4.3%, respectively. However, and even for high RCA replacement levels (RCA100%), all RAC slabs met the deflection requirements in BS 8110. Additional tests are necessary to confirm these findings and evaluate the long-term (>90 days) performance of composite slabs cast with RCA.
- Results from human-induced vibration tests showed that the RAC slabs met the requirements in ISO 2631-2:2003 and ISO

4866:2010. For slab RCA100%, the frequencies for normal walking (5.15-5.78 Hz), brisk walking (8.28-8.95 Hz) and jumping (10.08-10.12 Hz) remained within an acceptable range of comfort for occupants.

- For the slabs tested in this study, the FEA results agreed well (within an accuracy of 2 to 5%) with the experimental results, thus suggesting that Abaqus® is suitable to simulate the flexural capacity of the tested RAC slabs. An average FEA Prediction/Test ratio of 0.97 also indicate that the numerical models captured very well the dynamic behaviour of the tested slabs. This confirms the suitability of the modelling approach adopted in the FEA the tested slabs.

- The results from the parametric analyses on Abaqus® showed that an increase in span length decreased the first natural frequency of the RAC slabs. To meet the serviceability criteria in ACI 318, the span length of slabs with a 100% RCA replacement level should be below 12 m, and the slabs should also have a deck depth above 125 mm. Further parametric analyses are required to examine other case studies different to those investigated in this study.

- Overall, the results of this study confirm that high levels of RCA replacement can be used in the design and construction of composite slabs. Nonetheless, further tests and analysis on composite slabs with other types of RAC and other geometries should be carried out to confirm the findings presented in this study.

Acknowledgments

This work was supported by Walailak University Graduate Scholarships (Contract No. CGS-RF-2566-13). This research was also supported by Thailand Science Research and Innovation Fund Contract No. FRB660041/0227. The authors also acknowledge the support provided by the Capacity Enhancement and Driving Strategies for Bilateral and Multilateral Cooperation for 2021 (Thailand and UK). The fourth author thanks the support provided by the Academy of Medical Sciences through the 'Capacity and capability building to develop recycled aggregate concrete in South East Asia' (project GCRFNGR7\1344).

Conflict of Interest

There is no conflict of interest.

Supporting Information

Applicable.

References

- [1] A. B. Idrus, J. B. Newman, Construction related factors influencing the choice of concrete floor systems, *Construction*

- Management and Economics*, 2002, **20**, 13-19, doi: 10.1080/01446190110101218.
- [2] Y. Feng, Y. Su, N. Lu, S. Shah, Meta concrete: exploring novel functionality of concrete using nanotechnology, *Engineered Science*, 2019, **8**, 1-10, doi: 10.30919/es8d816.
- [3] I. M. Ahmed, K. Daniel Tsavdaridis, The evolution of composite flooring systems: applications, testing, modelling and eurocode design approaches, *Journal of Constructional Steel Research*, 2019, **155**, 286-300, doi: 10.1016/j.jcsr.2019.01.007.
- [4] N. C. Tuan, D. Dang Tung, Experimental studies of the reusable steel deck forms for concrete slabs, *IOP Conference Series: Materials Science and Engineering*, 2023, **1289**, 012030, doi: 10.1088/1757-899x/1289/1/012030.
- [5] H. Zhang, Y. Geng, Y.-Y. Wang, X.-Z. Li, Experimental study and prediction model for bond behaviour of steel-recycled aggregate concrete composite slabs, *Journal of Building Engineering*, 2022, **53**, 104585, doi: 10.1016/j.job.2022.104585.
- [6] W. Li, J. Xiao, C. Shi, C. S. Poon, Structural behaviour of composite members with recycled aggregate concrete—an overview, *Advances in Structural Engineering*, 2015, **18**, 919-938, doi: 10.1260/1369-4332.18.6.919.
- [7] L. J. Hu, Y. H. Chui, D. M. Onysko, Vibration serviceability of timber floors in residential construction, *Progress in Structural Engineering and Materials*, 2001, **3**, 228-237, doi: 10.1002/pse.69.
- [8] T. M. Murray, D. E. Allen, E. E. Ungar, Floor Vibrations Due to Human Activity, *American Institute of Steel Construction*, 1997.
- [9] L. Alberto López Ruiz, X. Roca Ramón, S. Gassó Domingo, The circular economy in the construction and demolition waste sector - A review and an integrative model approach, *Journal of Cleaner Production*, 2020, **248**, 119238, doi: 10.1016/j.jclepro.2019.119238.
- [10] B. Wang, L. Yan, Q. Fu, B. Kasal, A comprehensive review on recycled aggregate and recycled aggregate concrete, *Resources, Conservation and Recycling*, 2021, **171**, 105565, doi: 10.1016/j.resconrec.2021.105565.
- [11] H. M. S. C. H. Bandara, G. Thushanth, H. M. C. C. Somarathna, D. H. G. A. E. Jayasinghe, S. N. Raman, Feasible techniques for valorisation of construction and demolition waste for concreting applications, *International Journal of Environmental Science and Technology*, 2023, **20**, 521-536, doi: 10.1007/s13762-022-04015-z.
- [12] R. P. Neupane, T. Imjai, N. Makul, R. Garcia, B. Kim, S. Chaudhary, Use of recycled aggregate concrete in structural members: a review focused on Southeast Asia, *Journal of Asian Architecture and Building Engineering*, 2023, 1-24, doi: 10.1080/13467581.2023.2270029.
- [13] J. Yang, Q. Du, Y. Bao, Concrete with recycled concrete aggregate and crushed clay bricks, *Construction and Building Materials*, 2011, **25**, 1935-1945, doi: 10.1016/j.conbuildmat.2010.11.063.
- [14] T. Ozbakkaloglu, A. Gholampour, T. Xie, Mechanical and durability properties of recycled aggregate concrete: effect of recycled aggregate properties and content, *Journal of Materials in Civil Engineering*, 2018, **30**, 04017275, doi: 10.1061/(asce)mt.1943-5533.0002142.
- [15] S.C. Kou, C.S. Poon, Enhancing the durability properties of concrete prepared with coarse recycled aggregate, *Construction and Building Materials*, 2012, **35**, 69-76, doi: 10.1016/j.conbuildmat.2012.02.032.
- [16] Ö. Çakır, Experimental analysis of properties of recycled coarse aggregate (RCA) concrete with mineral additives, *Construction and Building Materials*, 2014, **68**, 17-25, doi: 10.1016/j.conbuildmat.2014.06.032.
- [17] N. Kachouh, H. El-Hassan, T. El-Maaddawy, Effect of steel fibers on the performance of concrete made with recycled concrete aggregates and dune sand, *Construction and Building Materials*, 2019, **213**, 348-359, doi: 10.1016/j.conbuildmat.2019.04.087.
- [18] N. Kachouh, H. El-Hassan, T. El-Maaddawy, Influence of steel fibers on the flexural performance of concrete incorporating recycled concrete aggregates and dune sand, *Journal of Sustainable Cement-Based Materials*, 2021, **10**, 165-192, doi: 10.1080/21650373.2020.1809546.
- [19] N. Makul, R. Fediuk, M. Amran, A.M. Zeyad, A. R. de Azevedo, S. Klyuev, N. Vatin, M. Karelina, Capacity to develop recycled aggregate concrete in South East Asia, *Buildings*, 2021, **11**, 234, doi: 10.3390/buildings11060234.
- [20] B. Cantero, M. Bravo, J. de Brito, I. F. Sáez del Bosque, C. Medina, Mechanical behaviour of structural concrete with ground recycled concrete cement and mixed recycled aggregate, *Journal of Cleaner Production*, 2020, **275**, 122913, doi: 10.1016/j.jclepro.2020.122913.
- [21] V. W. Y. Tam, M. Soomro, A. C. J. Evangelista, A review of recycled aggregate in concrete applications (2000-2017), *Construction and Building Materials*, 2018, **172**, 272-292, doi: 10.1016/j.conbuildmat.2018.03.240.
- [22] N. Makul, R. Fediuk, M. Amran, A.M. Zeyad, S. Klyuev, I. Chulkova, T. Ozbakkaloglu, N. Vatin, M. Karelina, A. Azevedo, Design strategy for recycled aggregate concrete: A review of status and future perspectives, *Crystals*, 2021, **11**, 695, doi: 10.3390/cryst11060695.
- [23] M. Setkit, S. Leelatanon, T. Imjai, R. Garcia, S. Limkatanyu, Prediction of shear strength of reinforced recycled aggregate concrete beams without stirrups, *Buildings*, 2021, **11**, 402, doi: 10.3390/buildings11090402.
- [24] Y. Zhu, W. Jian, W. Cao, T. Shao, Research on flexural performance of high-strength recycled concrete composite slabs. Proceedings of the 22nd national conference on structural engineering, 2012, **2**, 197-201.
- [25] H. Zhang, Y.-Y. Wang, Q. Wang, Y. Geng, Experimental study and prediction model for non-uniform shrinkage of recycled aggregate concrete in composite slabs, *Construction and Building Materials*, 2022, **329**, 127142, doi: 10.1016/j.conbuildmat.2022.127142.
- [26] H. Zhang, Y. Geng, Y. Y. Wang, X. Z. Li, Experimental study and prediction model for bond behaviour of steel-recycled aggregate concrete composite slabs, *Journal of Building Engineering*, 2022, **53**, 104585, doi: 10.1016/j.job.2022.104585.

- [27] S. Avudaiappan, E. I. Saavedra Flores, G. Araya-Letelier, W. Jonathan Thomas, S. N. Raman, G. Murali, M. Amran, M. Karelina, R. Fediuk, N. Vatin, Experimental investigation on composite deck slab made of cold-formed profiled steel sheeting, *Metals*, 2021, **11**, 229, doi: 10.3390/met11020229.
- [28] X. Cui, J. Zhang, W. Cao, Flexural performance analysis of profiled steel plate-recycled concrete composite plate, In Proceedings of the 24th National Conference on Structural Engineering, 2015, **1**, 342-347.
- [29] Q. Wang, J. Yang, Y. Liang, H. Zhang, Y. Zhao, Q. Ren, Prediction of time-dependent behaviour of steel-recycled aggregate concrete (RAC) composite slabs via thermo-mechanical finite element modelling, *Journal of Building Engineering*, 2020, **29**, 101191, doi: 10.1016/j.jobe.2020.101191.
- [30] M. Plos, J. Shu, K. Zandi, K. Lundgren, A multi-level structural assessment strategy for reinforced concrete bridge deck slabs, *Structure and Infrastructure Engineering*, 2017, **13**, 223-241, doi: 10.1080/15732479.2016.1162177.
- [31] T. Imjai, R. Garcia, B. Kim, C. Hansapinyo, P. Sukontasukkul, Serviceability behaviour of FRP-reinforced slatted slabs made of high-content recycled aggregate concrete, *Structures*, 2023, **51**, 1071-1082, doi: 10.1016/j.istruc.2023.03.075.
- [32] S. Leelatanon, T. Imjai, M. Setkit, R. Garcia, B. Kim, Punching shear capacity of recycled aggregate concrete slabs, *Buildings*, 2022, **12**, 1584, doi: 10.3390/buildings12101584.
- [33] T. Imjai, F. Kefyalew, P. Aosai, R. Garcia, B. Kim, H. M. Abdalla, S. N. Raman, A new equation to predict the shear strength of recycled aggregate concrete Z push-off specimens, *Cement and Concrete Research*, 2023, **169**, 107181, doi: 10.1016/j.cemconres.2023.107181.
- [34] M. M. Orvin, K. A. Anik, Minimum slab thickness requirement of RCC Slab in order to prevent undesirable floor vibration, *International Journal of Advances in Mechanical and Civil Engineering*, 2016, **3**, 2394-2827.
- [35] ISO 2631-1:1997/Amd 1:2010, Mechanical vibration and shock: Evaluation of human exposure to whole-body vibration, *International Standard Organization*, 2010, **2**, 1-6.
- [36] C. J. Middleton, J. M. W. Brownjohn, Response of high frequency floors: a literature review, *Engineering Structures*, 2010, **32**, 337-352, doi: 10.1016/j.engstruct.2009.11.003.
- [37] ASTM International Committee C09 on Concrete and Concrete Aggregates, Standard test method for compressive strength of cylindrical concrete specimens. *ASTM international*, 2014.
- [38] ASTM Subcommittee C09.61 on Testing for Strength, ASTM C39/C39M-21, Standard Test Method for Compressive Strength of Cylindrical Concrete Specimens, *American Concrete Institute*, 2021, doi: 10.1520/C0039_C0039M-21.
- [39] ASTM International Committee C496/C496M-11, Standard test method for splitting tensile strength of cylindrical concrete specimens, *ASTM International*, 2011.
- [40] ASTM International Committee C78/C78M-18, Standard test method for flexural strength of concrete (using simple beam with third-point loading), *ASTM International*, 2002, pp.1-3.
- [41] ASTM Committee A-01 on Steel, Stainless Steel and Related Alloys. Standard test methods and definitions for mechanical testing of steel products, *ASTM International*, 2017.
- [42] T. Alkhrdaji, E. R. Fyfe, V. M. Karbhari, M. Schupack, C. E. Bakis, A. Ganjehlou, J. G. Korff, D. W. Scott, P. N. Balaguru, D. J. Gee, M. W. Lee, *ACI 440.3 R-04: Guide Test methods for fiber-reinforced polymers (FRPs) for reinforcing or strengthening concrete structures*. American Concrete Institute, 2004.
- [43] American Concrete Institute committee ACI 318-14, *Building Code Requirements for Structural Concrete*. American Concrete Institute, 2014.
- [44] S.-H. Lee, K.-K. Lee, S.-S. Woo, S.-H. Cho, Global vertical mode vibrations due to human group rhythmic movement in a 39 story building structure, *Engineering Structures*, 2013, **57**, 296-305, doi: 10.1016/j.engstruct.2013.09.035.
- [45] S. Shahid, A. Nandy, S. Mondal, M. Ahamad, P. Chakraborty, G. C. Nandi, A study on human gait analysis, Proceedings of the Second International Conference on Computational Science, Engineering and Information Technology. October 26 - 28, 2012, Coimbatore UNK, India. New York: ACM, 2012, 358-364, doi: 10.1145/2393216.2393277.
- [46] G. A. Cavagna, M. Mantovani, P. A. Willems, G. Musch, The resonant step frequency in human running, *Pflügers Archiv*, 1997, **434**, 678-684, doi: 10.1007/s004240050451.
- [47] British Standard committee BS 6472-1, Guide to evaluation of human exposure to vibration in buildings. Vibration sources other than blasting, *British Standard*, 2008.
- [48] ISO committee 2631-2, Mechanical vibration and shock evaluation of human exposure to whole-body vibration - Part 2: Vibration in buildings (1 Hz to 80 Hz), *ISO standard*, 2003, **2**, 1-11.
- [49] BSI Group, BS ISO 4866, Mechanical vibration and shock, Vibration of fixed structures, Guidelines for the measurement of vibrations and evaluation of their effects on structures, *British Standard*, 2010.
- [50] ISO committee 2631-1, Mechanical vibration and shock evaluation of human exposure to whole-body vibration: Part 1: General requirements, *ISO standard*, 1997.
- [51] H. Al Ajmani, F. Suleiman, I. Abuzayed, A. Tamimi, Evaluation of concrete strength made with recycled aggregate, *Buildings*, 2019, **9**, 56, doi: 10.3390/buildings9030056.
- [52] L. Butler, J. S. West, S. L. Tighe. Effect of recycled concrete coarse aggregate from multiple sources on the hardened properties of concrete with equivalent compressive strength, *Construction and Building Materials*, 2013, **47**, 1292-1301, doi: 10.1016/j.conbuildmat.2013.05.074.
- [53] J. K. Wight, F. G. Barth, R. J. Becker, K. B. Bondy, J. E. Breen, J. R. Cagley, M. P. Collins, W. G. Corley, C. W. Dolan, A. E. Fiorato, C. E. French, *ACI Committee 318, Building Code Requirements for Structural Concrete (ACI 318-05) and commentary (ACI 318R-05)*. Am. Concr. Institute, Farmingt. Hills, MI, 430, 2003.
- [54] Canadian Standards Association, *Design of concrete structures*, *Canadian Standard*, 2004
- [55] British Standard committee BS 8500-2:2015, *Concrete-*

Complementary British Standard to BS EN 206–1–Part 2: Specification for Constituent Materials and Concrete, *British Standard*, 2015, doi: 10.3403/BS8500

[56] T. Li, J. Xiao, T. Sui, C. Liang, L. Li, Effect of recycled coarse aggregate to damping variation of concrete, *Construction and Building Materials*, 2018, **178**, 445-452, doi: 10.1016/j.conbuildmat.2018.05.161.

[57] B. Davis, D. Liu, T. M. Murray, Simplified experimental evaluation of floors subject to walking-induced vibration, *Journal of Performance of Constructed Facilities*, 2014, **28**, 04014023, doi: 10.1061/(asce)cf.1943-5509.0000471.

[58] G. Abaqus, Abaqus 6.11. Dassault Systemes Simulia Corporation, 2011.

[59] British Standards Institution, Eurocode 2: Design of concrete structures: Part 1-1: General rules and rules for buildings, British Standards, 2004.

[60] R. Mast, Vibration of precast prestressed concrete floors, *PCI Journal*, 2001, **46**, 76-86.

[61] E. Hamdy, O. Abdulghafour, A. Abdulghafour, Optimum design and efficiency of one-way slab according to ACI, *International Research Journal of Engineering and Technology*, 2001.

Publisher's Note: Engineered Science Publisher remains neutral with regard to jurisdictional claims in published maps and institutional affiliations.